Analyst

Cite this: *Analyst*, 2012, **137**, 1205

www.rsc.org/analyst

PAPER

Quantum-dot-based biosensor for simultaneous detection of biomarker and therapeutic drug: first steps toward an assay for quantitative pharmacology

Chi Yang,[a] Chunxiang Xu,*[a] Xuemei Wang[a] and Xiao Hu[b]

Received 25th September 2011, Accepted 27th November 2011
DOI: 10.1039/c2an15894a

Quantitative pharmacology (QP) is often used to study the recommended dose of a drug. Using colorectal cancer as a model, the relationship between exposure (cetuximab, C225, therapeutic drug of colorectal cancer) and the biomarker response (carcinoembryonic antigen, CEA, biomarker of colorectal cancer) is the core for the QP of C225. Thus, simultaneous detection of CEA and C225 is the first step towards an assay for the QP of C225. We developed a quantum dot (QD)-based multi-analyte biosensor for the simultaneous determination of CEA and the corresponding therapeutic drug C225. The assay is based on the competition between a quantum-dots-labeled glycans and target glycans using lectins as the recognition element. The dual-analytic biosensor detected CEA and C225 in the range from 1 ng mL^{-1} to 400 μg mL^{-1} by stripping voltammetry. The biosensor developed here for the simultaneous detection of the biomarkers and therapeutic drugs is expected to develop as a potential technique for quantitative pharmacology.

Introduction

Quantitative pharmacology (QP) can be applied in all stages of preclinical and clinical drug development through analysis on the dynamic changes of the therapeutic drugs and biomarkers (indicating the risk of the disease) in the plasma of patients.[1–3] At the preclinical stage, potential applications might comprise the evaluation of the identification of bio-/surrogate markers, as well as dosage optimization. At the clinical stage, analytical quantitative pharmacology applications include characterization of the dose–concentration–effect/toxicity relationship, evaluation of age and gender effects.[2,3] Through an intrinsic understanding of the quantitative pharmacology above, the simultaneous quantitation of biomarker and drug is important. So far, the conventional methods (such as high performance liquid chromatography,[4] fluorometry[5,6] and radioimmunoassay[7,8]) for probing biomarker and drug are time-consuming and expensive, and sophisticated instruments and technical expertise required.[9] Furthermore, it is difficult for these methods to obtain the concentration of the biomarker and drug after a single run. Therefore, an effective, simple, rapid and simultaneous detection in a single run is critically required.

Quantum-dots (QDs), owing to their unique properties,[10] have been used often in multiplexed bioanalysis.[11–15] Recently, many QD-based (such as ZnS, CdS, and PbS) multi-analyte biosensing methods have been developed to simultaneously determine the multiple DNA/cancer biomarker analytes,[14,15] but few of them have been reported for the simultaneous quantitation of biomarker and drug. To find the optimal dose (cetuximab, C225) for individual colorectal cancer patients, the relationship between exposure (C225) and the magnitude of biomarker (CEA, biomarker of the colorectal cancer) response is often gained by quantitative pharmacology studies. So, the dynamic changes of CEA and C225 should be known in advance, and a multi-analyte biosensing method for the simultaneous determination of CEA and C225 is greatly desired.[16–18] In this paper, the biomarker of CEA and the corresponding therapeutic drug C225 were selected as a proof-to-concept and were detected simultaneously by the QD-based multi-analyte biosensor after a single run. The method described here is expected to expand the application of the biosensor.

Experimental

Materials

CEA and C225 were purchased from Sigma Aldrich. Concanavalin A (Con A), and *Euonymus europaeus* lectin (EEL), a carbohydrate-free protein, were purchased from Sigma Aldrich and Vector to act as special recognition elements for CEA and for C225, respectively. Prostate specific antigens (PSA), immunoglobulin G (IgG) and other reagents, proteins solvents were purchased from Sigma Aldrich. Stock solutions were prepared using deionized water. The ZnO QDs and 11-mercaptoundecanoic acid stabilized CdSe QDs were prepared using a synthetic route reported earlier.[19–21] Owing to Zn^{2+} and $Zn(OH)^{+}_{(aq)}$ ions in the surface of the ZnO QDs,[22] the ZnO/CEA bioconjugates could

[a]*State Key Laboratory of Bioelectronics, School Electronic Science and Engineering, Southeast University, Nanjing, 210096, P. R. China. E-mail: xcxseu@seu.edu.cn; Fax: +86-25-83790755*
[b]*School of Material Science and Engineering, Nanyang Technological University, Singapore 639798*

be formed through electrostatic interaction between the positively charged ZnO QDs surface and the negatively charged CEA ending groups.[15,23] The COOH ligand capped CdSe could be broken down into negative COO^- under given conditions[21] and the conjugation of CdSe/C225 is carried out by mixing the solutions of *N*-(3-dimethylamminopropyl)-*N*′-ethylcarbodiimide hydrochloride and *N*-hydroxysulfosuccinimide sodium salt.[14]

Apparatus

The morphology and size of the ZnO and CdSe QDs were analyzed with a transmission electron microscope (TEM, JEM-100S, JEOL, Japan). Fourier transform infrared (FTIR) spectroscopy measurements were carried out using an Edinburgh FLS 920, LSM510 laser confocal fluorescence microscope, and Nicolet 380, respectively. All the Circular Dichroism (CD) spectra were taken using a Jasco J-725S spectropolarimeter fitted with a 150-W xenon lamp. Quartz cells of 1-mm optical path length were used for all CD measurements of proteins (C225 and CEA) and protein/QD solutions, and the spectra were recorded in the far-UV region (190–250 nm) with a response time of 8-s intervals and scan speed of 50 nm min^{-1}.

All electrochemical measurements were carried out using a CHI 830 electrochemical workstation (Shanghai, China) with a three-electrode system, in which a platinum coil, calomel (saturated KCl) and the glassy-carbon disk ($\varnothing = 3$ mm) electrode acted as the auxiliary electrode, reference electrode and working electrode, respectively.

Preparation of the sensor

The fabrication and sensing processes are illustrated in Scheme 1. In step (a), the glass surfaces was aldehyde-activated[24] and then the lectin layer of Con A and EEL was covalently assembled by soaking the aldehyde-activated samples in an electrolytic cell with 50 μL lectins for 12 h at 4 °C, followed by removal of the solution and washing with water. The surface of the glass substrates was then blocked through treatment with 50 μL 10 mM PBS (pH7.4) containing 1% (w/v) bovine serum albumin (BSA) solution for 2 h, and then washing with water.

In step (b), the lectin-modified glass substrates were incubated in 50 μL 10 mM PBS (pH 7.0) solution of ZnO and CdSe QD-bioconjugates for 2 h to assemble a layer of QD-bioconjugates on the lectin surface. After thorough washing, the captured QD-bioconjugates on the glass surface was observed through fluorescence images, as shown in Fig. 1a.

In Scheme 1 step (c), the samples were further incubated for 2 h in 50 μL solution with the desired amount of the analyte protein (C225, CEA or mixture) at room temperature. The samples were washed twice with 100 μL deionized water and once with 100 μL of 10 mM PBS (pH 7.4) buffer. In this case, the analyte molecules were loaded on the substrate and the corresponding QD-bioconjugates were supplanted out because the tagged protein has a significantly lower affinity for the lectin compared to the unmodified analyte.[14,25] The fluorescence became weaker after the analyte C225 molecules were added as compared before. (Fig. 1b *vs.* Fig. 1a) This indicated that some CdSe/C225 bioconjugates were successfully replaced by the analyte C225.

Electrochemical measurements

As shown in step (d) of Scheme 1, Zn^{2+} and Cd^{2+} ions in the remnant QD-bioconjugates were dissolved in 2000 μL, 0.01 M HCl solution with sonication for 15 min. Subsequently, the solution was transferred to an 8 mL electrochemical glass cell containing 2000 μL of 10 mM PBS (pH 7.0) buffer spiked with 10 ppm mercury(II). And then the solution was adjusted to pH 6.15 by NaOH solution (80 μL, 0.32 M). The electrochemical stripping detection involved a 1 min pretreatment at +0.6 V, and 2 min electrodeposition at −1.3 V, and stripping from −1.3 V to

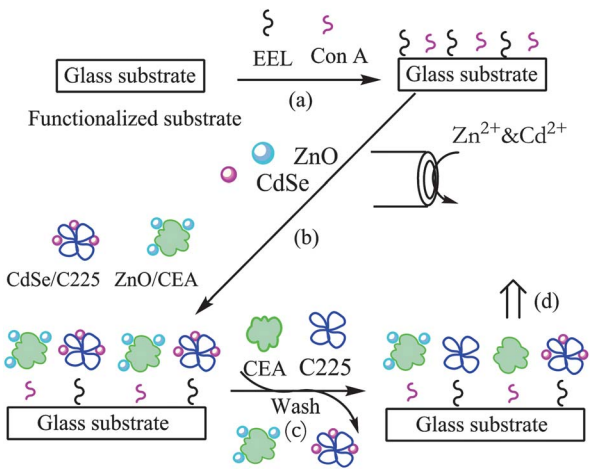

Scheme 1 Fabrication and sensing process of ZnO and CdS QD-based biosensor for simultaneous detection of CEA and C225. (a) Substrate functionalization and lectins (EEL and Con A) immobilization; (b) assembly of bioconjugates (ZnO/CEA and CdSe/C225) on lectin layer; (c) analytes addition and displacement; and (d) SWV detection of the remnant QDs.

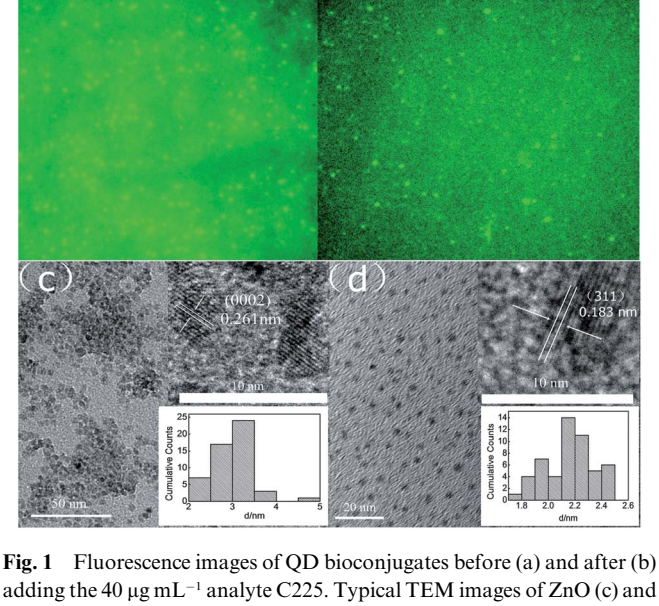

Fig. 1 Fluorescence images of QD bioconjugates before (a) and after (b) adding the 40 μg mL^{-1} analyte C225. Typical TEM images of ZnO (c) and CdSe (d) QDs inserted with the corresponding high resolution TEM image and statistical size distribution.

−0.4 V using a square-wave voltammetric waveform, with 4 mV potential steps, 25 Hz frequency and 25 mV amplitude.

Results and discussion

Fig. 1 shows typical TEM images of QDs and the statistical size distribution. The images reveal the uniform size of the QDs. The size statistic demonstrates that the diameter of ZnO and CdSe QDs are mainly distributed over 3∼3.5 nm with an average value of 3 nm (Fig. 1c) and 2.1∼3.2 nm with an average value of 2.3 nm (Fig. 1d), respectively. Using the high-resolution image the interplanar spacing for the ZnO and CdSe QDs were found to be 0.261 nm and 0.183 nm, respectively (inserted image in Fig. 1c and Fig. 1d). These values correspond to the interplanar distance of ZnO (0001) and CdSe (311) planes (JCPDS19-191). Further XRD structural analysis of the QDs is shown in Fig. 2a. The broad peak is derived from ZnO (JCPDS36-1451) and the diffraction appearing at 25.2, 42.3, and 49.7 correspond to the (111), (220), and (311) planes of cubic CdSe (JCPDS19-191), which was consistent with the analysis of HRTEM results above. A homogeneous solution of QDs was shown in the inserted image in Fig. 2b, which indicated that the as-prepared quantum dots were stable in the PBS (pH = 7.0) solution.

The PL spectra of the QDs are also shown in Fig. 2b. The PL of the ZnO QDs presents a strong broad green defect-related emission at 550 nm and a weak ultraviolet interband emission at 367 nm. The narrow green spectrum at 550 nm originates from the interband emission of the CdSe QDs. These results are consisted with the observation from the fluorescence images described above (Fig. 1a,b). The intrinsic emission of both ZnO and CdSe QDs presents the blue-shift relative to the corresponding bulk semiconductor, which is suggested to originate from QDs with a small size where the quantum confinement effect can work well.[26,27]

CD spectroscopy is a widely used technique to analyze secondary structure and to monitor the structural changes occurring in proteins in response to external factors.[28] The QD-bioconjugates stock solution (protein [C225 and CEA] concentration = 15 μM mL^{-1}, protein/QD = 5 : 1 molar ratio, 600 μL) was prepared and used for the preparation of CD samples. As described above, the QD-bioconjugates is formed through self-assembly, electrostatic interaction between the negatively charged QDs surface, and the positively charged protein ending groups. Fig. 3a shows the CD spectra of protein (C225) and QD-bioconjugates. Before the conjugation, the spectra of C225 showed two strong double minima at 228 and 209 nm and a stronger maximum at 191 nm, which is typical of high α-helical content.[28] The crossover point at 200 nm was also assigned to the α-helix structure. The 209-nm peak has a larger intensity than the 228-nm peak, showing that the 35% C225 is more like an α/β type.[28] After the conjugation with QDs, the CD spectrum looked similar, but the difference between the two minima became less obvious. This indicated a decrease in the percentage of α-helices. The positive peak only shifted slightly from 193 to 191 nm, indicating that there was no significant change in the secondary structure of C225. The intensities of the negative peak decreased, and the peak at 228 nm shifted to 219 nm, which may

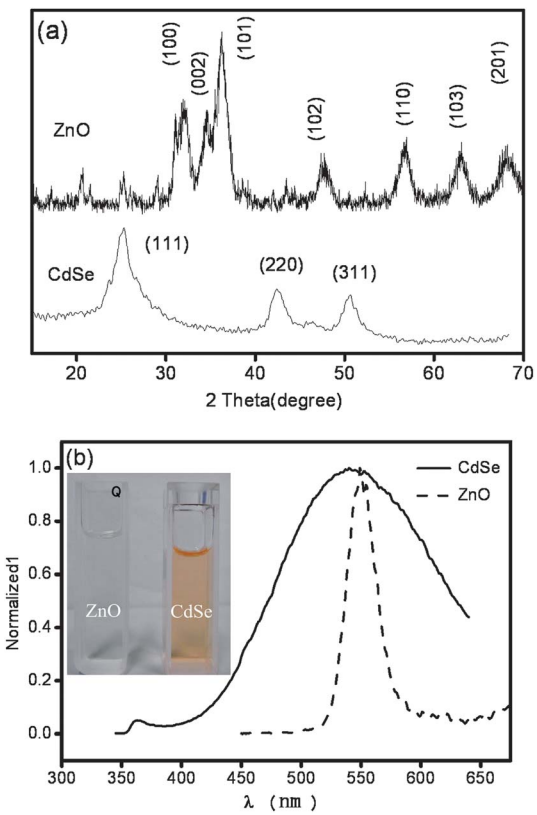

Fig. 2 XRD of the as-prepared QDs (a) and PL spectra of QDs, inserted with the QDs in PBS (pH = 7) solution (b).

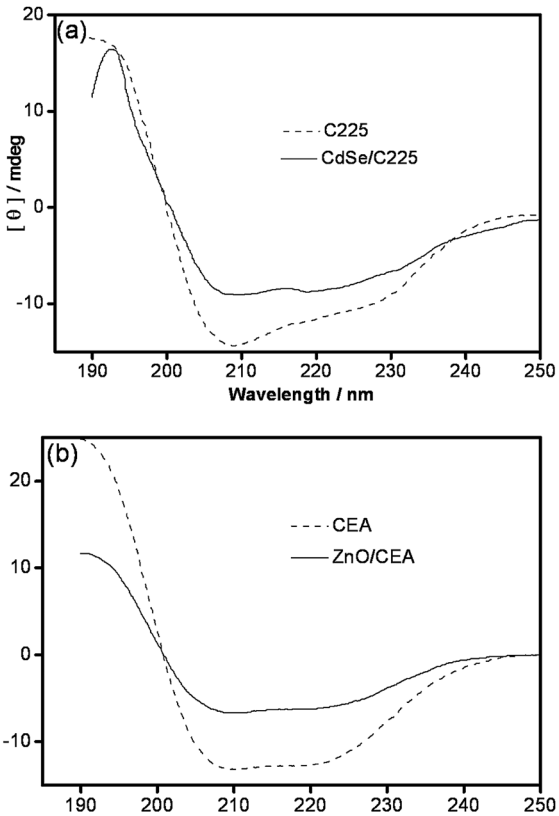

Fig. 3 CD spectra of pure C225 and QD/C225 bioconjugates (a) and CEA and QD/CEA bioconjugates (b).

result from a slight change of secondary structure of C225.[28] Although a slight change of secondary structure of C225 occurred during the formation of bioconjugates according to the CD spectroscopic data, the previous fluorescence study of CdSe/C225 biosensors indicated that this small change did not inhibit the activity of C225. A similar phenomenon was also found and reported by Zhang *et al.*[29] when they conjugated the protein trichosanthin to the surface of core/shell QDs.

As for the ZnO/CEA bioconjugates, there is no change of secondary structure of CEA occurring during the formation of bioconjugates according to the CD spectroscopic data (Fig. 3b), which was consistent with the biocompatibility of ZnO results.[30]

As described above, the analyte proteins were held on the substrate and the corresponding QD-bioconjugates were displaced due to the labelled proteins has a significantly lower affinity for the lectin compared to the unmodified analyte.[9,18,31] It is obvious that the concentration of the analyte proteins related to the displaced QD-bioconjugates. So, the concentration of the analyte proteins could be determined by monitoring the displaced QD-bioconjugates. Here, we detected the electrochemical SWV of the remaining QD-bioconjugates on the substrate instead of the displaced QD-bioconjugates. In this case, the low concentration of the replaced bioconjugates corresponds to the high concentration of the remaining QD-bioconjugates, so it is expected to improve signal response and signal-to-noise ratio for low-concentration detection. Single-analyte sensing was used first to assess the selectivity of the biosensor.

Fig. 4A shows the typical square-wave voltammetry (SWV) curves of the metal ions from the residual QDs in the undisplaced bioconjugates when the single-analyte C225 was added with different concentrations of 0 (a), 100 (b), and 400 (c) μg mL^{-1}. The well-defined electrochemical stripping peak (1) at ~1.09 V and peak (2) at ~0.67 V just correspond to current response of Zn^{2+} and Cd^{2+} from the undisplaced ZnO/CEA and CdSe/C225, respectively. The SWV signal of Cd^{2+} obviously reduces with increase of the target concentration of C225 while the signal of Zn^{2+} almost remains at the same level. The remarkably high selectivity also reflects the presence of numerous QDs per labelled protein molecule. Fig. 4B shows voltammograms for a blank solution (a), as well as for 500 μg mL^{-1} non-target PSA (b) and IgG (c). As desired, there is no current response, even as their relatively high concentration (b and c *vs.* a). For comparison, the well defined response to C225 observed in Fig. 4A(b). These experiments confirmed that the assay systems were performing correctly and that there was no cross-reactivity between lectins and non-target proteins.

A key advantage of the multi-analyte biosensor is its potential application in quantitative pharmacology. Using colorectal cancer as a model, C225 has been designed to specifically block epidermal growth factor receptor (EGF) expression, which has emerged as an important therapeutic target in colorectal cancer. Levels of CEA would predict therapeutic response towards anti-EGF therapy by C225 in colorectal cancer.[32] After administering the C225, the CEA level would be down-regulated. The optimum dose of the C225 could be achieved once we know the relationship between CEA and C225. Thus, simultaneous detection of CEA and C225 is the first step toward an assay for the quantitative pharmacology of C225. To demonstrate the simultaneous detection in a single run, CEA and C225 were selected as a proof-

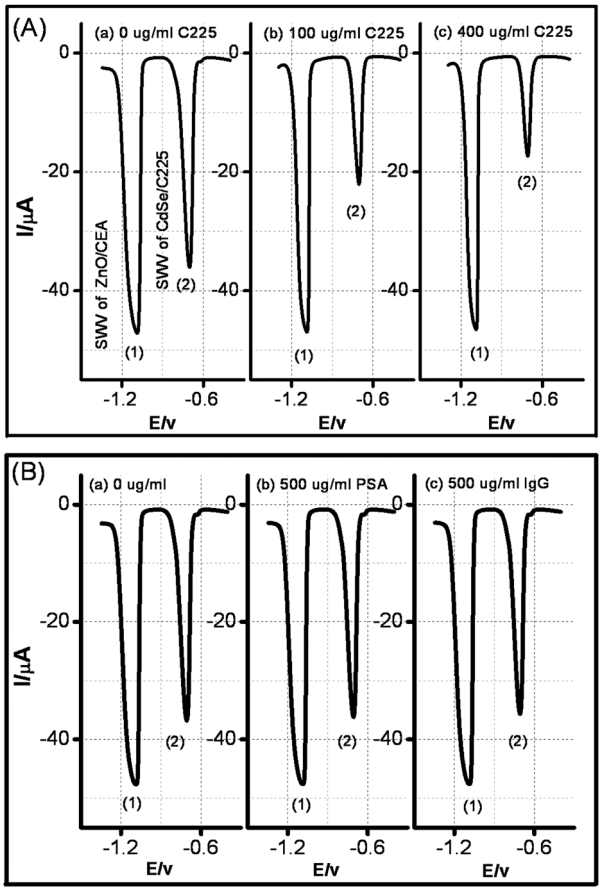

Fig. 4 (A) Typical SWV curves for ZnO and CdSe QD-bioconjugates after the addition of single analyte C225 with concentrations of 0 (a), 100 (b), and 400 (c) μg mL^{-1}. (B) SWV response of CEA (1) and C225 (2) after additions of non-target proteins: (a) blank, (b) 500 μg mL^{-1} PSA, (c) 500 μg mL^{-1} IgG.

to-concept and detected by the biosensor. As shown in Scheme 1, it is illustrated for the dual-analyte detection of CEA (1) or C225 (2) in connection with ZnO and CdSe quantum tracers, respectively, along with the co-immobilization of the corresponding lectins. The position and size of the corresponding metal peaks reflect the identity and concentration of the corresponding analyte protein. For example, additions of CEA or C225 resulted in substantial (20 and 32%) diminutions of the corresponding zinc and cadmium peaks (Fig. 5A(b) and Fig. 5A(c), respectively, *vs.* Fig. 5A(a)). No apparent change in the response of the second label is observed, indicating negligible cross-interferences. In contrast, the simultaneous addition of both proteins resulted in similar reductions of both metal peaks (Fig. 5A(d)). The zinc and cadmium peaks are sharp and well resolved. Fig. 5B further plots the relationship between the response current on the concentration of the coexistent analytes at a concentration range of 10 ng mL^{-1} to 400 μg mL^{-1}. The curves were not linear, as are commonly observed for displacement assays,[33] and we used curve-fitting for the calibration procedure. The limits of detection at a signal-to-noise ratio of three for CEA and C225 were 0.31 ng mL^{-1} and 3.4 μg mL^{-1}, respectively. The cut-off values of the coexistent analytes in clinical diagnosis are 5 ng mL^{-1} and 50 μg mL^{-1},[34,35] respectively. Therefore, the sensitivity and

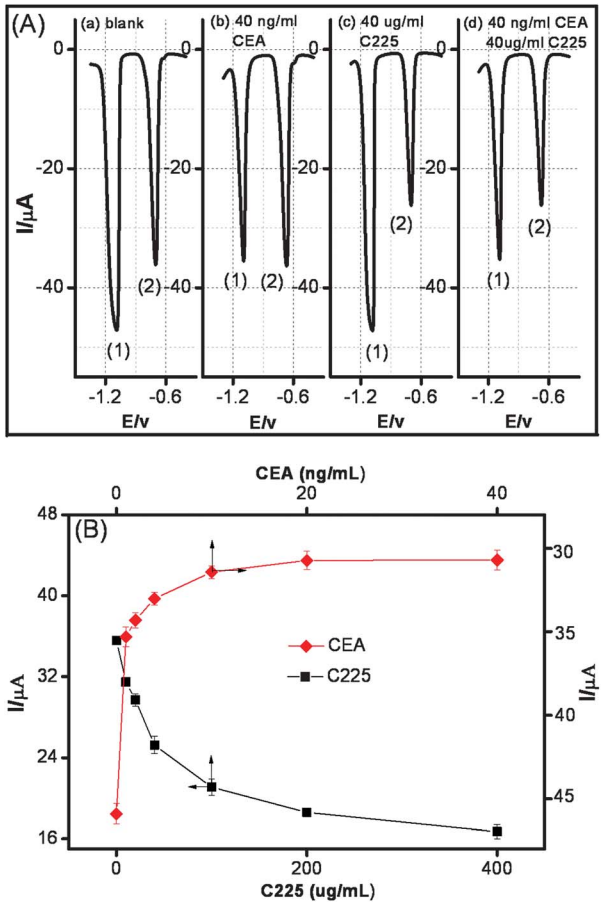

Fig. 5 (A) Typical SWV signals for simultaneous detected of CEA (1) and C225 (2) after the addition of (a) 0 ng mL^{-1} protein, (b) 40 ng mL^{-1} CEA, (c) 40 μg mL^{-1} C225, and (d) a mixture of 40 ng mL^{-1} CEA and 40 μg mL^{-1} C225. (B) The calibrated plot of response current *vs.* analyte concentration. Error bars indicate the standard deviation for the mean of three measurements.

detection ranges of our suspension array were enough for practical application. Up to 5–6 analyte proteins are thus expected to be measured simultaneously in a single run, based on the number of non-overlapping metal peaks.

Conclusions

In summary, we have developed a biosensor for dual-analyte detection using ZnO and CdSe quantum dots. The biomarker of CEA for colorectal cancer and the corresponding therapeutic drug C225 were selected as a proof-to-concept and detected simultaneously in a single run. The sensitive and selective of such a multi-analyte biosensing method opens up the possibility of using biosensor for simultaneous bioelectronic detection of biomarkers and therapeutic drugs. It is expected to be applied as a tool for quantitative pharmacology studies.

Acknowledgements

This work was supported by NSFCs (60725413, 60976002), '973' Program (2011CB302004 and 2007CB936300) and MOE (309015).

References

1 R. Miller, W. Ewy, B. W. Corrigan, D. Ouellet, D. Hermann, K. G. Kowalski, P. Lockwood, J. R. Koup, S. Donevan, A. El-Kattan, C. S. Li, J. L. Werth, D. E. Feltner and R. L. Lalonde, *J. Pharmacokinet. Pharmacodyn.*, 2005, **32**, 185–197.
2 L. Zhang, V. Sinha, S. T. Forgue, S. Callies, L. Ni, R. Peck and S. R. Allerheiligen, *J. Pharmacokinet. Pharmacodyn.*, 2006, **33**, 369–393.
3 H. Derendorf, L. J. Lesko, P. Chaikin, W. A. Colburn, P. Lee, R. Miller, R. Powell, G. Rhodes, D. Stanski and J. Venitz, *J. Clin. Pharmacol.*, 2000, **40**, 1399–1418.
4 R. G. Kay, C. Barton, C. P. Velloso, P. R. Brown, C. Bartlett, A. J. Blazevich, R. J. Godfrey, G. Goldspink, R. Rees, G. R. Ball, D. A. Cowan, S. D. Harridge, J. Roberts, P. Teale and C. S. Creaser, *Rapid Commun. Mass Spectrom.*, 2009, **23**, 3173–3182.
5 I. Hemmila and S. Webb, *Drug Discovery Today*, 1997, **2**, 373–381.
6 A. Eggert, N. Haubner, S. Klausch, U. Karsten and R. Schumann, *Biofouling*, 2006, **22**, 79–90.
7 J. Landon and A. C. Moffat, *Analyst*, 1976, **101**, 225–243.
8 O. A. Naik George and W. Moe Gordon, *Clin. Chem. Lab. Med.*, 2007, **45**, 1353–1359.
9 Z. L. Yao, B. T. Zhao, E. P. Hoffman, S. Ghimbovschi, D. C. DuBois, R. R. Almon and W. J. Jusko, *Pharm. Res.*, 2007, **24**, 643–653.
10 J. Wang, *Small*, 2005, **1**, 1036–1044.
11 M. Y. Han, X. H. Gao, J. Z. Su and S. H. M. Nie, *Nat. Biotechnol.*, 2001, **19**, 631–635.
12 J. Wang, G. Liu and A. Merkoci, *J. Am. Chem. Soc.*, 2003, **125**, 3214–3215.
13 G. D. Liu, J. Wang, J. Kim, M. R. Jan and G. E. Collins, *Anal. Chem.*, 2004, **76**, 7126–7130.
14 J. A. Hansen, J. Wang, A.-N. Kawde, Y. Xiang, K. V. Gothelf and G. Collins, *J. Am. Chem. Soc.*, 2006, **128**, 2228–2229.
15 I. L. Medintz, H. T. Uyeda, E. R. Goldman and H. Mattoussi, *Nat. Mater.*, 2005, **4**, 435–446.
16 S. Hammarstrom, E. Engvall, B. G. Johanssont, S. Svenssont, G. Sundblad and I. J. Goldstein, *Proc. Natl. Acad. Sci. U. S. A.*, 1975, **72**, 1528–1532.
17 C. H. Chung, B. Mirakhur and E. Chan, *N. Engl. J. Med.*, 2008, **358**, 1109–1117.
18 C. P. Swaminathan, N. Surolia and A. Surolia, *J. Am. Chem. Soc.*, 1998, **120**, 5153–5159.
19 D. L. Klayman and T. S. Griffin, *J. Am. Chem. Soc.*, 1973, **95**, 197–199.
20 B. X. Gu, C. X. Xu, G. P. Zhu, S. Q. Liu, L. Y. Chen, M. L. Wang and J. J. Zhu, *J. Phys. Chem. B*, 2009, **113**, 6553–6557.
21 M. J. Mulvihill, S. E. Habas, I. Jen-La Plante, J. Wan and T. Mokari, *Chem. Mater.*, 2010, **22**, 5251–5257.
22 A. Degen and M. Kosec, *J. Eur. Ceram. Soc.*, 2000, **20**, 667–673.
23 B. X. Gu, C. X. Xu, C. Yang, S. Q. Liu and M. L. Wang, *Biosens. Bioelectron.*, 2011, **26**, 2720–2728.
24 O. Krishnamoorthy, T. Bei and E. Zoumakis, *Biosens. Bioelectron.*, 2006, **22**, 707–714.
25 J.-P. Chen, *J. Chem. Tech. Biotechnol.*, 1993, **56**, 213–211.
26 N. W. Wang, Y. H. Yang and G. W. Yang, *Nanoscale Res. Lett.*, 2011, **6**, 338–344.
27 Y. Yan, Z. M. Liao, Y. Q. Bie, H. C. Wu, Y. B. Zhou, X. W. Fu and D. P. Yu, *Appl. Phys. Lett.*, 2011, **99**, 103103–103106.
28 G. D. Fasman, *Circular Dichroism and the Conformational Analysis of Biomolecules*, Plenum Press, 1996.
29 C. Y. Zhang, H. Ma, S. M. Nie, Y. Ding, L. Jin and D. Y. Chen, *Analyst*, 2000, **125**, 1029–1031.
30 Z. Li, R. S. Yang, M. Yu, F. Bai, C. Li and Z. L. Wang, *J. Phys. Chem. C*, 2008, **112**, 20114–20117.
31 J. Wang, Z. Dai, A.-N. Kawde, Y. Xiang, J. T. La Belle, J. Gerlach, V. P. Bhavandan, S. Svarovsky and L. Joshi, *Nanomed.: Nanotechnol., Biol. Med.*, 2006, **2**, 314–317.
32 G. Folprecht, J. Tabernero, C. H. Köhne, C. Zacharchuk, L. Paz-Ares, F. Rojo, S. Quinn, E. Casado, R. Salazar, R. Abbas, C. Lejeune, I. Marimón, J. Andreu, U. Ubbelohde, H. Cortes-Funes and J. Baselga, *Clin. Cancer Res.*, 2008, **14**, 215–223.
33 J.-P. Chen, *J. Chem. Tech. Biotechnol.*, 1993, **56**, 213–211.
34 J. J. Che, H. Wang, Z. H. Chen, X. Li, Y. Hou, C. Q. Shan and Y. G. Cheng, *J. Pharm. Biomed. Anal.*, 2009, **50**, 183–188.
35 P. Norouzi, V. K. Gupta, F. Faridbod, B. Larijani and M. R. Ganjali, *Anal. Chem.*, 2011, **83**, 1564–1570.